Surface roughening with quenched disorder in high dimensions: Exact results for the Cayley tree

Sergey V. Buldyrev,[1] Shlomo Havlin,[1,2] Janos Kertész,[3,4] Reza Sadr-Lahijany,[1] Arkady Shehter,[2] and H. Eugene Stanley[1]

[1] *Center For Polymer Studies and Department of Physics, Boston University, Boston, Massachusetts 02215*

[2] *Department of Physics, Bar Ilan University, Ramat Gan, Israel*

[3] *Isaac Newton Institute for Mathematical Sciences, Cambridge University, Cambridge, United Kingdom*

[4] *Institute of Physics, Technical University, Budapest, Budafoki ut 8, H-1111, Hungary*

(Received 21 February 1995)

Discrete models describing pinning of a growing self-affine interface due to geometrical hindrances can be mapped to the diode-resistor percolation problem in all dimensions. We present the solution of this percolation problem on the Cayley tree. We find that the order parameter P_∞ varies near the critical point p_c as $\exp(-A/\sqrt{p_c - p})$, where p is the fraction of bonds occupied by diodes. This result suggests that the critical exponent β_p of P_∞ diverges for $d \to \infty$, and that there is no finite upper critical dimension. The exponent $\nu_\parallel$ characterizing the parallel correlation length changes its value from $\nu_\parallel = \frac{3}{4}$ below p_c to $\nu_\parallel = \frac{1}{4}$ above p_c. Other critical exponents of the diode-resistor problem on the Cayley tree are $\gamma = 0$ and $\nu_\perp = 0$, suggesting that $\nu_\perp/\nu_\parallel \to 0$ when $d \to \infty$. Simulation results in finite dimensions $2 \leq d \leq 5$ are also presented.

PACS number(s): 64.60.Ak,47.55.Mh,68.3.Fx

I. INTRODUCTION

Kinetic roughening during growth of interfaces has attracted considerable recent interest [1]. One of the most challenging problems in this context is the role of quenched disorder. Several experiments have been carried out [2–4], and the roughness was found to be anomalous in the sense that the measured roughness exponent α differed from that predicted by the Kardar-Parisi-Zhang (KPZ) equation [5]. Several theoretical attempts have been undertaken to explain this discrepancy based either on continuum equations of surface growth including quenched randomness [6] or on a simple geometrical picture where pinning is attributed to percolative blockades [3,4,7]. The relation between these two approaches was discussed by Amaral *et al.* [8].

For simplicity, we first discuss the case of 1+1 dimensions. The initially flat fluid surface is hindered in its motion by randomly distributed quenched obstacles. In order to maintain the experimentally observed absence of overhangs in the model, the fluid is supposed to flow back very fast if it manages to overcome an obstacle. Therefore the motion of the interface is stopped only if a (directed) percolation path of obstacles spans the sample. The roughness exponent α of the resulting pinned interface can be calculated by using the well known numerical values of the directed percolation correlation length exponents and the resulting value of the roughness exponent is in good agreement with experimental observations [2–4].

Recently it was shown [4] that a three-dimensional generalization of the model is able to describe experimental results in 2+1 dimensions as well. This result, together with theoretical interest about the high-dimensional behavior of kinetic roughening, motivate the present investigation [6]. First we show that the $(d+1)$-dimensional generalization of the model of pinning by geometric blockades becomes a percolation model of d-dimensional hypersurfaces with no overhangs. This model is dual to the random network of resistors and diodes [9]. After showing this duality, we give the solution of the diode-resistor percolation (DRP) problem on the Cayley tree [10], which is expected to exhibit the infinite-dimensional behavior.

II. DIODE-RESISTOR PERCOLATION MODEL

Let us first recall the directed percolation depinning (DPD) model in its simplest form in 1+1 dimensions. We start from the single step model [11], where growth proceeds on a square lattice tilted by 45° and fluid penetrates from the bottom to the top (Fig. 1). The surface height h is a single-valued function of the coordinate x and it is initially flat. The surface width

$$w \equiv \sqrt{\langle h^2 \rangle - \langle h \rangle^2} \tag{1a}$$

grows in time, where here the angular brackets denote an average over space and/or realizations of quenched noise. The fluid occupies the cells and spreads by breaking through the walls separating the cells.

In the present model (which differs from the original definition of the single step model [11]), all cells at the interface between occupied and unoccupied regions are simultaneously updated. Without disorder, our model is a trivial system where the interface moves with a constant velocity and remains parallel to its initial position. The disorder is introduced on the walls of the cells in the following way: all walls are permeable from above but there is a certain fraction of walls chosen at random with probability p that are blocking flow from below (see Fig. 1). Due to this randomness the interface roughens

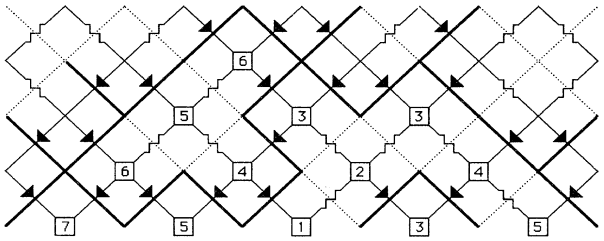

FIG. 1. Diode-resistor network as a model of fluid propagation. Solid lines represent blocking obstacles that stop fluid from below. Dotted lines are cell walls permeable from below. Squares with numbers inside represent wet cells together with the time step they become wet. Initially only one cell, marked by "1," was wet. Note that solid lines do not stop the fluid propagation from above in the direction pointed by diodes. The wetting process is stopped by a spanning path of directed percolation that starts at the bottom left and ends at the bottom right corner of the lattice. In a multidimensional space this path becomes a spanning directed surface that consists of blocking facets, perpendicular to the diodes.

while propagating upwards. In the stationary regime, the surface can be characterized by a roughness exponent α:

$$w \sim L^{\alpha}, \tag{1b}$$

where L is the system size.

At sufficiently high density of obstacles the surface becomes completely pinned. Denoting the blocking walls by directed bonds (say, from left to right), the motion of the fluid is stopped whenever a spanning directed (bond) percolation path across the sample occurs. The directedness of the pinning path is a consequence of the suppression of overhangs achieved in the model. We always allow penetration of the fluid from above, even if there is an obstacle hindering the flow upward. This model of pinning represents a class of models of growth in disordered media, all belonging to the same universality class [3,7]. In the above version the parameter p controls the model and critical behavior is obtained at a special value of $p = p_c$. Versions of the model where the criticality is built up in a self-organized way have been constructed by applying ideas of invasion directed percolation [3,7] or gradient percolation [8].

The generalization of the model to $d+1$ dimensions is straightforward. At $t = 0$ the d-dimensional interface is flat and coincides with the "horizon" hyperplane $x_1 + x_2 + \cdots + x_d = 0$. The fluid now occupies the cells of a hypercubic lattice and flows through the facets of the cells, which are permeable from above but blocked from below with probability p. The object blocking the motion of the interface is now a single-valued simply connected d-dimensional surface consisting of the blocked facets and does not have overhangs with respect to the direction of growth given by the vector $(1, 1, \ldots, 1)$. We call this surface a *directed percolating surface.*

Let us define the dual lattice in the usual way. The centers of the cells are connected by bonds normal to the facets. The structure created this way is again a hypercubic lattice. The dual problem of the directed surface percolation model is defined by the following rule: *A dual bond is occupied by a diode pointing downward if the facet is blocked and it is occupied by a resistor if the facet is permeable in both directions.* As long as there is a simply connected directed hypersurface in the directed problem, percolation upward—above this hypersurface—is impossible on the dual lattice. Equivalently, if percolation upward is possible, there must be holes on any directed spanning surface. Thus the model of diode-resistor percolation [12] is dual to the model of the surface pinned by geometrical hindrances, and the motion of the fluid can be thought of as taking place on the dual lattice.

From the theoretical point of view, it is important to study the dependence of the exponents on the dimensionality and to find the upper critical dimension above which the behavior becomes trivial (mean-field-like). Several controversial suggestions have been put forward to answer these questions for the problem of interface pinning by quenched disorder [6]. From the discussion above it follows that this problem is equivalent to DRP. Therefore it would be of interest to see how the exponents of DRP behave as a function of the dimensionality.

The equivalence between the directed percolation and the DRP was first established by Dhar *et al.* [9] in 1+1 dimensions. In $d+1$ dimension, the directed surface can be considered a d-dimensional generalization of the path of directed percolation. The equivalence between directed surface percolation and DRP can also be considered as the directed analog of the duality between conventional bond percolation and percolation of simply connected hypersurfaces [13]. In the latter problem, the correlation length characterizing the clusters of isotropic percolation is the same as correlation length characterizing their surfaces, both diverging at the same critical threshold. We develop this analogy in the directed case.

To proceed we first define the clusters of the DRP. This is nontrivial since—as one can always move downward in this system—the number of sites that can be reached from a chosen site is always infinite. Thus a cluster at any given site cannot be identified with the set of sites made wet by a fluid pumped at that site. Instead, we define the cluster with respect to a site (the origin) as the set of points which can be reached from it without using bonds below the horizon, the hyperplane $x_1 + x_2 + \cdots + x_d = 0$. As long as $p > p_c$ the clusters defined this way remain finite. They are hill shaped and they have a characteristic height $\xi_{\perp}$ and a characteristic width $\xi_{\parallel}$. Such a hill will just fit into a "cupola" of the percolating hypersurface. Therefore the characteristic lengths of the hypersurface should be equal to those of the DRP clusters:

$$\xi_{\perp} \sim |p - p_c|^{-\nu_{\perp}}, \tag{2}$$

$$\xi_{\parallel} \sim |p - p_c|^{-\nu_{\parallel}}. \tag{3}$$

These equations lead to the following expression for the roughness of the pinned interface:

$$\alpha = \nu_{\perp}/\nu_{\parallel}. \tag{4}$$

TABLE I. Critical exponents of the diode-resistor problem in finite dimensions.

d	$1+1$	$2+1$	$3+1$	$4+1$	Cayley tree
α	0.63 ± 0.01	0.48 ± 0.03	0.38 ± 0.04	0.27 ± 0.05	0
β_p	0.7 ± 0.1	1.65 ± 0.2	2.0 ± 0.3	2.2 ± 0.3	∞
γ_p	2.00 ± 0.05	1.31 ± 0.05	0.88 ± 0.1	0.65 ± 0.10	0
τ	1.28 ± 0.02	1.52 ± 0.03	1.65 ± 0.05	1.70 ± 0.20	2
$\nu_\perp$	1.09 ± 0.01	0.58 ± 0.06	0.3 ± 0.1	0.2 ± 0.1	0
$\nu_\parallel$	1.73 ± 0.01	1.18 ± 0.05	0.86 ± 0.1	0.6 ± 0.2	1/4

How the exponents depend on the dimension and what the upper critical dimension is (above which the behavior becomes mean-field-like) are questions of great theoretical interest.

In kinetic surface roughening these questions have been rather controversial. Also, for the pinning problem several suggestions have been put forward [6] implying different high-dimensionality behavior. Therefore it would be of interest to see how the pinning model equivalent of DRP behaves as a function of dimensionality.

We have carried out extensive numerical simulations and calculated the dimension-dependent exponents. The results are summarized in Table I. The exponents do not seem to have reached asymptotic values even in dimensions as high as $4+1$. Thus it is not yet clear what the upper critical dimension for the DRP problem is. The general way to answer this question is to construct a mean-field theory and to consider the importance of the fluctuations in the Ginzburg sense. Such a consideration leads to upper critical dimension 6 for bond percolation [14] (the dual to hypersurface percolation) or to $4+1$ for directed percolation [15]. Another, usually equivalent way is to identify the upper critical dimension with the dimension where the hyperscaling relation is fulfilled with the mean-field exponents [12]. For the directed percolation problem the hyperscaling law is

$$1/\sigma + \beta_p = (d-1)\nu_\perp + \nu_\parallel, \tag{5}$$

where $1/\sigma$ is the exponent of the singularity of a typical cluster size s_c near the critical point

$$s_c \sim |p - p_c|^{-1/\sigma}, \tag{6}$$

and β_p describes the behavior of the probability P_∞ of a randomly taken point to belong to a percolating cluster

$$P_\infty \sim |p - p_c|^{\beta}. \tag{7}$$

Hyperscaling relation has simple geometrical meaning. The characteristic volume v_c encapsulating the cluster is proportional to the product of the correlation lengths

$$v_c \sim \xi_\perp^{d-1}\xi_\parallel. \tag{8}$$

On the other hand, the *ramified* cluster of directed percolation occupies only s_c cells of the total number of cells v_c of the characteristic volume. The geometrical probability s_c/v_c is the probability P_∞ of a point to belong to a typical cluster, percolating the volume v_c. Thus

$$s_c \sim \xi_\perp^{d-1}\xi_\parallel P_\infty. \tag{9}$$

Using Eq. (9) together with Eqs. (2), (3), (6), and (7) we get Eq. (5). In our case, however, a cluster is the compact object, confined between an initial horizontal plain and a directed surface that stops its growth. Thus $s_c = v_c$ and the hyperscaling relation acquires a simpler form

$$1/\sigma = (d-1)\nu_\parallel + \nu_\perp \tag{10}$$

without an extra term β_p and $\nu_\parallel$ and $\nu_\perp$ exchanging their places.

Note that $1/\sigma = \beta_p + \gamma_p$, where γ_p describes the divergence of the average cluster size

$$\langle s \rangle \sim |p - p_c|^{-\gamma_p}. \tag{11}$$

Numerical data for the critical exponents in $d \geq 2$ presented in Table I (see also [16]) suggest that β_p is much larger and γ_p is much smaller than the corresponding values for directed percolation. The values of γ_p for higher dimensions become less than one, which contradicts a recent conjecture [17] , according to which $\gamma_p = 1 + \nu_\perp$ in all dimensions. To determine the mean-field exponents in the following section we suggest a DRP model on a Cayley tree.

III. DIODE-RESISTOR PERCOLATION ON THE CAYLEY TREE

It is widely accepted that the Cayley tree mimics the infinite-dimensional behavior of the lattice systems because it cannot be embedded in any finite-dimensional lattice [14]. In order to illustrate our method of solving DRP on the Cayley tree, the analogous solutions of percolation and directed percolation problems on the Cayley tree are presented in in Appendixes A and C, respectively.

The first step is that the directed nature of the problem has to be implemented on the tree. This is an ambiguous procedure and the results might depend on it. Figure 2 illustrates our choice. We assign an altitude $i \geq 0$ to each site on the Cayley tree that has coordination number $z_c = 4$. In this way, each site at level i is connected via two bonds to a higher level $i+1$, and by two bonds to a lower level $i-1$ [10]. The sites at level $i = 0$ are connected only to the sites at level $i = 1$.

The bonds of the Cayley tree are occupied by diodes

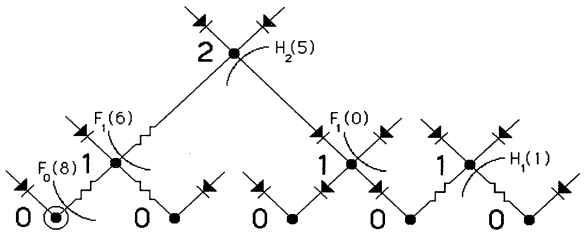

FIG. 2. A finite diode-resistor cluster of size $s = 9$ on the Cayley tree with coordination number $z_c = 4$. The initial site is marked by a larger circle. Sites are arranged vertically according to the number of the level they belong to. The lowest level has the number equal to zero. In order to illustrate the concept of a branch, we show several examples of branches of various sizes s outgoing from sites at different levels i. These branches are indicated by arcs and probabilities $F_i(s)$, $H_i(s)$. For example, the right branch that is connected to the site at level $i = 2$ from below consists of $s = 5$ sites. Diodes that are connected to the cluster by their lower end only represent a surface that stops percolation. These diodes are considered to be upper branches of zero mass, which always have probability $F_i(0) \equiv p$. Note that only three resistors (not five as shown) are necessary to create this cluster.

pointing to a lower level with probability p and by resistors with probability $1 - p$. There exists a diode-resistor percolation threshold, $p = p_c$, above which there is no current between a site at level $i = 0$ and a site at level $i = +\infty$. Below p_c there is a finite probability that a site at level $i = 0$ will be connected to $+\infty$ by a path of resistors and diodes on which current can flow from $i = 0$ to $i = +\infty$. We define a cluster with respect to a given site at level i as the set of sites that can be reached by a current starting at this site. We also define a cluster branch to be a set of sites that are connected to a given site through one of the adjacent bonds.

To find p_c and the critical behavior we define the following quantities. $F_i(s)$ is the probability that a site at level i is connected via an upper bond to a branch of size s, and $H_i(s)$ is the probability that a site at level i is connected via a lower bond to a branch of size s. As a boundary condition, we have

$$H_0(s) = 0 \quad \text{if} \quad s > 0, \qquad H_0(0) = 1. \tag{12}$$

We define the probability of an infinite branch at zero level as $F_0(\infty) \equiv P_\infty$. This is the probability that one can go infinitely far from the bottom line, i.e., $F_0(\infty)$ is the order parameter of the problem. The exponent β_p is then defined by

$$F_0(\infty) \sim (p_c - p)^{\beta_p}. \tag{13}$$

The probability of occurrence of an upper branch of size zero, $F_i(0)$, is equal to p for all i. This happens when the bond under consideration is blocked by a diode. Simple probabilistic reasoning leads to the following equations:

$$F_i(s) = (1-p) \sum_{s_1+s_2+s_3=s-1} F_{i+1}(s_1)F_{i+1}(s_2)H_{i+1}(s_3), \tag{14}$$

$$H_i(s) = \sum_{s_1+s_2+s_3=s-1} H_{i-1}(s_1)H_{i-1}(s_2)F_{i-1}(s_3). \tag{15}$$

With the help of the generating functions for $F_i(s)$ and $H_i(s)$ [18],

$$f_i(x) = \sum_{s=0}^{\infty}{}' F_i(s)x^s, \tag{16}$$

$$h_i(x) = \sum_{s=0}^{\infty}{}' H_i(s)x^s, \tag{17}$$

Eqs. (14) and (15) can be written in a more compact form:

$$f_i(x) = p + x(1-p)h_{i+1}(x)f_{i+1}^2(x), \tag{18}$$

$$h_{i+1} = xf_i(x)h_i^2(x). \tag{19}$$

The use of generating functions in the simple case of classical percolation is illustrated in Appendix A. The value of $f_i(1)$ [or $h_i(1)$] is the probability that a site is not connected to the infinite cluster through an upper (or lower) bond. Every site on the infinitely high level $i \to \infty$ is connected to the infinite cluster via a lower bond

$$\lim_{i\to\infty} h_i(1) = 0, \tag{20}$$

and the only chance that this site is not connected to the infinite cluster via an upper bond is that this bond is diode. This happens with probability p, that is,

$$\lim_{i\to\infty} f_i(1) = p. \tag{21}$$

These two limiting conditions together with the fact that $H_i(s)$ and $F_i(s)$ cannot be negative imply that, for $i \to \infty$, $H_i(s) \to 0$ for all $s \geq 0$, $F_i(s) \to 0$ for all $s > 0$, and $F_i(0) = p$. This in turn leads to

$$\lim_{i\to\infty} f_i(x) = p, \tag{22}$$

$$\lim_{i\to\infty} h_i(x) = 0, \qquad 0 \leq x \leq 1. \tag{23}$$

Let us define the function $g_i(x) = xh_i(x)$. From the initial conditions (12) for $h_0(x)$ we have $g_0(x) = x$. Hence the function $g_0(x)$ is equivalent to the independent variable x. The recurrence relations for the pair $(f_i(x), g_i(x))$ are

$$f_i(x) = p + (1-p)g_{i+1}(x)f_{i+1}^2(x), \tag{24a}$$

$$g_{i+1}(x) = f_i(x)g_i^2(x). \tag{24b}$$

For any given value of p and x Eqs. (24) have unique solution $f_0(x)$ determined by initial condition $g_0(x) = x$ and limits (22) and (23). Equations (24) do not contain x explicitly. Thus any pair $(f_i(x), g_i(x))$ can be regarded as the initial pair $(f_0(x'), g_0(x'))$ for a new value of independent variable x', which must be equal to $g_0(x')$ as mentioned above, i.e., $x' = g_0(x') \equiv g_i(x)$. Any two successive iterations $f_i(x)$ and $f_{i+1}(x)$ are equal to the values of the function $f_0(x_1)$ and $f_0(x_2)$ at some new values of independent variable $x_1 = g_i(x)$ and $x_2 = g_{i+1}(x)$. Due to Eq. (24b) $x_2 = x_1^2 f(x_1)$ and thus Eqs. (24) can be written down as a single functional equation for function $f_0(x)$,

$$f_0(x) = p + (1-p)x^2 f_0(x) f_0^2(x^2 f_0(x)). \tag{25}$$

IV. RESULTS

The solution of Eqs. (22)–(24) provides the full description of the problem. First we present the numerical result shown in Fig. 3. We obtain Fig. 3 by taking fixed values of p and x and iterating Eqs. (24) from some initial values $(\tilde{f}_0, \tilde{g}_0)$ to higher and higher successive iterations $(\tilde{f}_i, \tilde{g}_i)$. If $\tilde{f}_0$ is larger than the true value $f_0(x)$, then (for some i) $\tilde{f}_i$ becomes larger than 1, which does not make sense. Conversely, if $\tilde{f}_0 < f_0(x)$, then (for some i) $\tilde{f}_i$ becomes less than p, which leads to $\tilde{f}_{i+1}^2 < 0$ and makes further iterations impossible. Thus, using this dichotomy, it is easy to make $\tilde{f}_0$ close to $f_0(x)$ with any arbitrarily prescribed accuracy.

The curves in Fig. 3 are parametrized by p. For p larger than a critical value p_c, i.e., when the concentration of diodes is high enough, the probability that a site at level 0 is not connected to infinity is 1. Thus the lines for $p > p_c$ are intersecting at the fixed point $f_0(1) = 1$, for which the order parameter $P_\infty = F_0(\infty) = 1 - f_0(1)$ is zero. However, for $p < p_c$ the lines are not intersecting each other and are crossing the straight line $x = 1$ at values $f_0(1)$ that are less than 1. This indicates that for $p < p_c$ the order parameter P_∞ is greater than 0. Geometrically, any sequence of successive iterations (g_i, f_i) for fixed x corresponds to a sequence of points $(x_i, f_0(x_i))$ moving along the curve corresponding to the given value of p from right to left and approaching limiting values $(0, p)$.

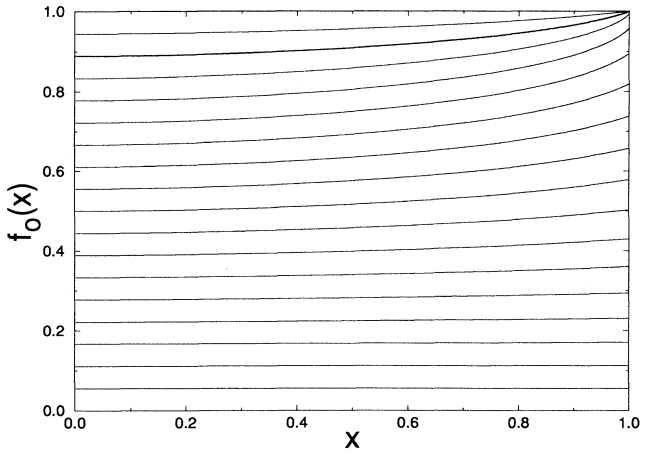

FIG. 3. Function $f_0(x)$ for different values of p computed numerically by the method explained in the article. The value of p for each graph can be seen from the value of the function at zero: $f_0(0) = p$. We see that the curves above the line $p = p_c = 8/9$ enter the point (1,1). Those with $p < p_c$ intersect the line $x = 1$ below 1, which means that the order parameter $p_0(\infty) = 1 - f_0(1)$ differs from zero. Every line enters $x = 1$ with a finite derivative, which means that the average cluster size always remains finite.

The behavior of the curves near $x = 1$ defines the critical behavior of the system. The average size of a branch connected to a site at level 0 can be defined from the slope of the curves at $x = 1$,

$$s_0 \equiv \sum_{s=1}^{\infty} F_0(s)s \Big/ \sum_{s=1}^{\infty} F_0(s) = \frac{\left[\frac{df_0(x)}{dx}\right]_{x=1}}{f_0(1)} = \left[\frac{d\ln f_0(x)}{dx}\right]_{x=1}. \tag{26}$$

The critical exponents of the problem can be obtained from the behavior of the function $f_0(x)$ near its fixed point $x = 1$. According to Tauberian theorems [19], this behavior defines the asymptotic form of the branch size distribution

$$F_0(s) \sim s^{-\tau}\phi(s/s_c), \tag{27}$$

where $\phi(x)$ is a cutoff function that exponentially goes to zero when $x \to \infty$, and s_c is the characteristic branch size: $s_c \sim |p - p_c|^{-1/\sigma}$.

Linearization of Eqs. (24) near the point (1,1) allows us to solve the problem analytically. First we obtain the critical probability $p_c = 8/9$ [20]. Next we find that the order parameter approaches 0 when $p \to p_c^-$ as

$$F_0(\infty) \sim \exp(-A_1/\sqrt{p_c - p}), \qquad A_1 = \frac{\pi\sqrt{2}\ln 3}{3}. \tag{28}$$

The analytical and numerical data are shown in Fig. 4. The rather unusual form of Eq. (28) has serious consequences. It is a much weaker singularity (an essential singularity) than those occurring at usual critical points [see Eq. (13)]. If we interpret Eq. (28) in terms of critical exponents we have

$$\beta_p = \infty \tag{29}$$

for the exponent of the order parameter.

Linearization also gives expressions for the average cluster size (see Fig. 5),

$$\langle s_0 \rangle = \frac{q - 5 - \sqrt{(q-9)(q-1)}}{4} = 1 - \varphi - \varepsilon \qquad (p > p_c), \tag{30}$$

$$\langle s_0 \rangle = \left(\frac{\ln q}{2}\frac{\varphi}{\theta} + 1 - \varepsilon\right) \Big/ f_0(1) \qquad (p < p_c), \tag{31}$$

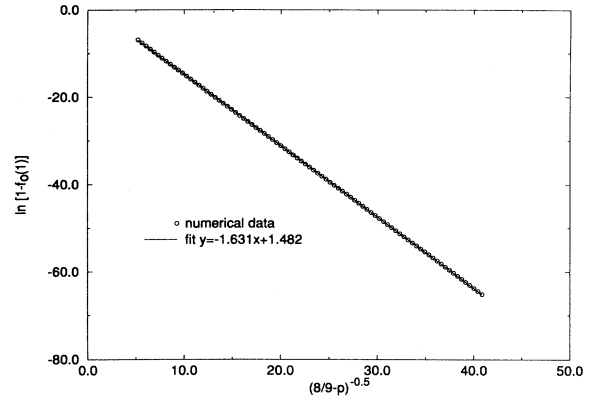

FIG. 4. Dependence of the logarithm of the order parameter $\ln F_0(\infty) \equiv \ln[1 - f_0(1)]$ on $1/\sqrt{p_c - p}$. The data are obtained by the same procedure as in Fig. 3. If Eq. (28) is correct, the data should follow a straight line with the slope $-A_1$. Fitted value $A_1 = 1.631$ coincides with the analytically computed one: $A_1 = (\pi\sqrt{2}\ln 3)/2$. Data span almost two orders of magnitude of $p_c - p$.

where $q = 1/(1 - p)$, $\varepsilon = (9 - q)/4$, $\varphi = \sqrt{|(9-q)(q-1)|}/4 = \sqrt{|2\varepsilon - \varepsilon^2|}$, and $\theta = \arcsin(\varphi/\sqrt{q})$. Equation (30) can be derived directly from (25) if one linearizes it near (1,1) [see also Eq. (B13)]. Equations (30) and (31) imply that the average cluster size is finite below and above p_c but has a first discontinuity at $p = p_c$, and consequently $\gamma_p = 0$.

Finally, using Tauberian theorems, we find that the exponents of the cluster size distribution are $\tau = 2$, $\sigma = 0$. In fact, for $p > p_c$, there is no apparent exponential cutoff in Eq. (27). Instead,

$$F_0(s) \sim \frac{1}{s^{\tau(p)}} \qquad (p > p_c), \tag{32}$$

where

$$\tau(p) = 1 + \frac{\ln \lambda_2}{\ln \lambda_1}, \qquad \lambda_{1,2} = \frac{3 - \varepsilon \pm \varphi}{q}, \tag{33}$$

or

$$\tau(p) \sim 2 + \frac{3\sqrt{2}}{\ln 3}|p - p_c|^{1/2}, \qquad p \to p_c^+. \tag{34}$$

Exactly at $p = p_c$

$$F(s) \sim \frac{1}{s^2 \ln^2 s} \qquad (p = p_c), \tag{35}$$

which is consistent with the fact that the average cluster size at $p = p_c$ remains finite.

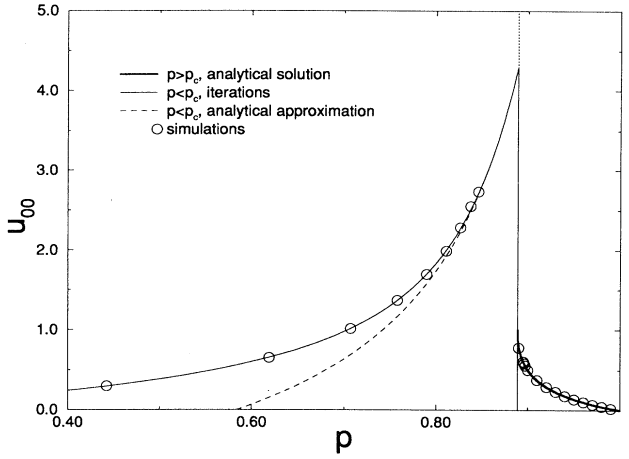

FIG. 5. Average size of the branches connected to level 0. The data for $p < p_c$ are obtained by iterating recurrent equations for average branch sizes u_{0i} and d_{0i} [see Eqs. (C31), (C45), (C46), and (C49) of Appendix C]. For $p > p_c$ the exact prediction of Eq. (30) is shown by bold solid line. For $p < p_c$ the prediction of Eq. (31) with $f_0(1)$ replaced by 1 is shown by dashed line. The results of computer simulations on the random diode-resistor Cayley tree are shown by circles and the results produced by Eq. (C49) by a solid line. The graph approaches $p = p_c$ with infinite derivative from above and with finite derivative from below and has a first order discontinuity at p_c.

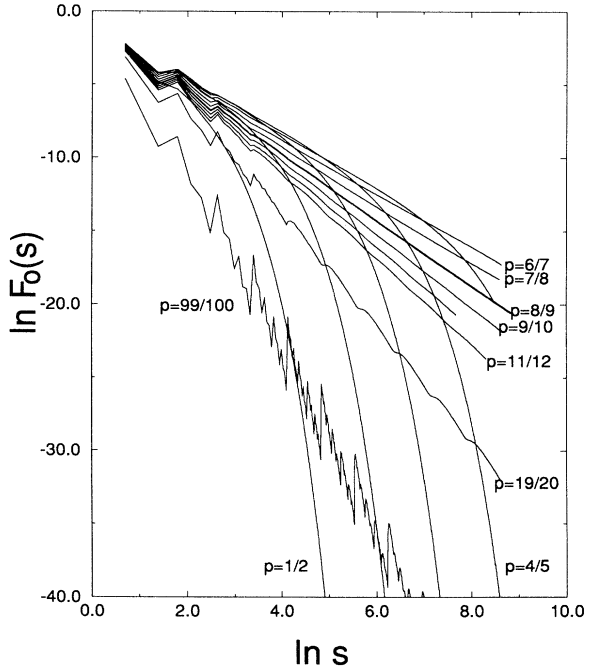

FIG. 6. Cluster size distribution for different values of p below and above $p_c = 8/9$ obtained by exact enumeration. We see that above p_c the curves can be approximated by power-law functions $F_0(s) \sim s^{-\tau}$ with exponent depending on p. At $p = p_c$, $\tau = 2$ and logarithmic corrections appear: $F_0(s) = s^{-2}\ln^{-2} s$. (The data for $p = p_c$ are shown by bold line.) For lines with $p < p_c$, a cutoff appears.

The apparent cutoff of the distribution appears below p_c:

$$s_c = \frac{e}{2}\frac{\sqrt{q}\ln q}{F_0(\infty)} \sim \exp(A_1/\sqrt{p_c - p}). \tag{36}$$

The numerical data, obtained directly from Eqs. (14)–(15), are in good agreement with the above analytical results (see Fig. 6). Complete derivations of Eqs. (27)–(35) are given in Appendix B.

In order to find the exponents $\nu_\perp$ and $\nu_\parallel$, we must compute correlation lengths of the problem. Using the analogy with directed percolation on the Cayley tree, we have done it in Appendix C. We show that $\xi_\perp$ remains finite and that $\xi_\parallel$ diverges as $|p - p_c|^{-1/4}$ above p_c,

$$\xi_\parallel^2 = \frac{q}{2\varphi} - \frac{q - 2 - 1/\langle s_0\rangle}{q - 1}, \tag{37}$$

but below p_c, $\xi_\parallel$ diverges as $|p - p_c|^{-3/4}$. Consequently,

$$\begin{aligned} \nu_\perp &= 0, \\ \nu_\parallel &= 1/4, \qquad p > p_c \\ \nu_\parallel &= 3/4, \qquad p < p_c. \end{aligned} \tag{38}$$

Hence the roughness exponent α defined by Eq. (1b) is $\nu_\perp/\nu_\parallel = 0$.

V. DISCUSSION

Since $\sigma = 0$ and $\nu_\parallel$ is finite, the hyperscaling relation Eq. (10) can be satisfied only if $d = \infty$. Hence we suggest that the critical dimension of the diode-resistor surface roughening problem is $d_c = \infty$. This means that for any finite dimension the roughness exponent α is positive and gradually approaches zero as $d \to \infty$.

This behavior is analogous to the behavior of the KPZ equation, for which it was proposed [21] that $\alpha \to 0$ as $d \to \infty$.

Other exponents measured numerically for higher dimensions seem to approach their values for the Cayley tree. (See Table I and tables in Ref. [22].) For example, γ_p gradually decreases and becomes less than one for higher dimensions, which contradicts recent conjecture [17] that $\gamma_p = 1 + \nu_\perp$ in all dimensions. On the other hand, τ gradually increases but always remains less than 2. An interesting observation is that the values of $\nu_\parallel$ for the Cayley tree are different above and below p_c and this has to be tested for the model in higher finite dimensions (the values of $\nu_\parallel$ in Table I are measured only for $p > p_c$). Also the results show discontinuities in the average height and average size at $p = p_c$. This may shed light on controversies regarding the values of α and $\nu_\parallel$ below p_c in low dimensions (see Makse and Amaral [24]).

The recent conjecture of Havlin *et al.* [23] that the upper critical dimension for the dynamical exponents of the surface growth problem in quenched disorder might be $d_c = 6$ does not contradict the above results. This is because the dynamical properties of the system which characterize growth only in the horizontal direction may be independent of geometrical properties of completely pinned clusters, which we study here. These geometrical properties describe only the completely stopped interface and they do not depend on the way this final stage is achieved.

ACKNOWLEDGMENTS

We wish to thank L. A. N. Amaral, A.-L. Barabási, S. T. Harrington, A. Ya. Kazakov, G. Huber, D. Stauffer, and T. Vicsek for helpful discussions, and NSF, Grant No. OTKA 1218 for financial support. J. K. is grateful to BU and to the Newton Institute for hospitality.

APPENDIX A: ILLUSTRATION OF THE METHOD FOR THE CLASSICAL CAYLEY TREE

First, let us show how the generating function approach works in the case of classical percolation on the Cayley tree [14] with coordination number $z_c = 3$, where the bonds are randomly disconnected with probability p. For each site we introduce a probability $F(s)$ that this site is connected to the branch of size s via a given bond. Since all branches and sites on this Cayley tree are equivalent, we can write

$$F(s) = (1-p)\sum_{s_1+s_2=s-1} F(s_1)F(s_2), \quad F(0) = p. \tag{A1}$$

This produces the generating function

$$f(x) = \sum_{s=0}^{\infty} F(s)x^s \tag{A2}$$

that satisfies the quadratic equation

$$f(x) = p + (1-p)xf^2(x), \tag{A3}$$

with two real solutions. Taking into account that if $x \le 1$ then $f(x) \le 1$, we select the smaller of the two solutions,

$$f(x) = \frac{1 - \sqrt{1 - 4p(1-p)x}}{2(1-p)x}. \tag{A4}$$

The order parameter is $P_\infty = 1 - f(1)$. At $x = 1$, the positive value of the square root is equal to $|2p - 1|$. If $p > 1/2$ then $|2p - 1| = 2p - 1$, which gives $f(1) = 1$. For p below $1/2$ we have $f(1) = p/(1-p) < 1$ and order parameter is different from zero. Hence $p_c = 1/2$ and

$$P_\infty = 1 - f(1) = \frac{1-2p}{1-p} \sim (p_c - p)^\beta, \tag{A5}$$

with $\beta = 1$. The function $f(x)$ has a singularity at point $x_0 = 1/4p(1-p)$ of the type

$$f(x) = A + B|x - x_0|^a, \tag{A6}$$

with $a = 1/2$. According to the Tauberian theorems [19], Eq. (A5) suggests that the Taylor expansion of the function $f(x)$ near $x = 0$ behaves as

$$F(s) = s^{-\tau}\phi(s^\sigma|p - p_c|) \sim s^{-\tau}\exp(-s/s_c), \tag{A7}$$

where

$$\tau = 1 + a, \qquad s_c = 1/\ln(x_0). \tag{A8}$$

Thus, in our case,

$$\tau = 3/2 \tag{A9}$$

and

$$s_c \approx \frac{1}{x_0 - 1} = \frac{p(1-p)}{(p - p_c)^2}, \tag{A10}$$

which gives

$$\sigma = 1/2. \tag{A11}$$

In this simple case the function $F(s)$ can be computed according to the binomial expansion of $\sqrt{1-y}$,

$$F(s) = 2p\frac{(2s-1)!!}{(2s+2)!!}[4p(1-p)]^s, \tag{A12}$$

where the ratio of factorials has the power-law asymptotic behavior $s^{-3/2}$, and the term $[4p(1-p)]^s$ gives an exponential cutoff.

We can also compute the average cluster size as the logarithmic derivative of $f(x)$ at $x = 1$ and get

$$\langle s\rangle = \frac{(1-p)}{2|p - p_c|}, \qquad p > p_c \tag{A13a}$$

$$\langle s\rangle = \frac{p}{2|p - p_c|}, \qquad p < p_c \tag{A13b}$$

which means that $\gamma = 1$ on both sides.

We can also consider a directed Cayley tree in which each site is located at a chemical distance i from the origin [10]. The chemical distance is defined as the number of bonds connecting the site to the origin. The level on this tree can be defined as a subset of sites with equal values of chemical distances i. For each level i, we can introduce the probabilities $F_i(s)$ that a site on this level is connected to a branch of size s. Then for the generating functions $f_i(x)$ we find

$$f_i(x) = p + (1-p)xf_{i+1}^2(x), \tag{A14}$$

which is analogous to Eqs. (24) in this simple case. In analogy with Eq. (24), by iterating Eq. (A14) we move f_i away from the fixed point $f(x)$ given in Eq. (A4). In principle, the value $f(x)$ can be defined by the same dichotomy rule as we use for finding the solution of Eqs. (24). Here, however, due to equivalence of all the levels, $f_{i+1} = f_i$, and we get the simple quadratic equation (A3) for the solution.

APPENDIX B: ANALYTICAL SOLUTION OF DIODE-RESISTOR PERCOLATION FOR CAYLEY TREE

As mentioned above, in the successive iterations of Eqs. (24) (g_i, f_i) are moving away from the fixed point $(1,1)$ towards their limiting point $(0,p)$. In order to study the vicinity of the fixed point, we must iterate Eqs. (24) backwards. Defining $x = g_{i+1}, y = f_{i+1}$ and $x' = g_i, y' = f_i$, we consider Eqs. (24) as a nonlinear transformation from unprimed quantities to primed,

$$y' = p + (1-p)xy^2, \tag{B1}$$

$$x' = \sqrt{\frac{x}{p + (1-p)xy^2}}. \tag{B2}$$

Successive application of these transformations moves the point (x,y) towards the fixed point $(1,1)$. Defining $\delta = 1 - x, \eta = 1 - y$, we linearize Eqs. (B1) and (B2) near the fixed point

$$\begin{pmatrix}\delta'\\ \eta'\end{pmatrix} = \mathcal{A}\begin{pmatrix}\delta\\ \eta\end{pmatrix}, \tag{B3}$$

with

$$\mathcal{A} = \frac{1}{q}\begin{pmatrix}(q-1)/2 & -1\\ 1 & 2\end{pmatrix}. \tag{B4}$$

Starting from any point with $\delta > 0, \eta > 0$ the successive iterations

$$\begin{pmatrix}\delta_n\\ \eta_n\end{pmatrix} = \mathcal{A}^n\begin{pmatrix}\delta\\ \eta\end{pmatrix} \tag{B5}$$

move towards the fixed point $(0,0)$. After finding the eigenvalues of the matrix $\mathcal{A}$, which are

$$\lambda_{1,2} = \frac{3 + q \pm \sqrt{(q-9)(q-1)}}{4q} \tag{B6}$$

$$= \frac{3 - \varepsilon \pm \varphi}{q} \tag{B7}$$

for $p \geq 8/9$, and

$$\lambda_{1,2} = \frac{3 - \varepsilon \pm i\varphi}{q} \tag{B8}$$

for $p \leq 8/9$, we can write down an explicit form of $\binom{\delta_n}{\eta_n}$. The crucial point of our analysis is the fact that $\lambda_{1,2}$ which are positive and less than unity for $p \geq 8/9$ become complex conjugate for $p < 8/9$. Thus the sequence $\binom{\delta_n}{\eta_n}$ approaches zero above $p = 8/9$ and below $p = 8/9$ in two different ways. Above $p = 8/9$, both δ_n and η_n remain positive for all n and their vector $\binom{\delta_n}{\eta_n}$ enters the fixed point along the eigenvector $\vec{v}_1 = \binom{1-\varepsilon+\varphi}{1}$ which corresponds to the largest eigenvalue $\lambda_1 = \frac{3-\varepsilon+\varphi}{q}$. This means that $x' \to 1$ (and $y' \to 1^-$) and consequently

$f_0(1) = 1^-$. Hence the order parameter $F_0(\infty) = 1 - f_0(1)$ is zero, which implies the absence of percolation above p_c.

Below p_c, the vector $\binom{\delta_n}{\eta_n}$ rotates around 0. Thus δ_n becomes negative for certain n, which is unphysical. The point at which x' becomes equal to 1 corresponds to $y' = f_0(1) < 1$. Thus for $p < 8/9$ we find a nonzero P_∞ and percolation occurs.

Hence we conclude that

$$p_c = 8/9. \tag{B9}$$

For $p > p_c$, after some algebra, we obtain

$$\delta_n = \frac{1}{2\varphi}[\lambda_1^n(\delta/s_0 - \eta) + \lambda_2^n(\eta - \delta s_0)], \tag{B10}$$

$$\eta_n = \frac{1}{2\varphi}[\lambda_1^n(\delta - \eta s_0) + \lambda_2^n(\eta/s_0 - \delta)], \tag{B11}$$

where $s_0 = 1 - \varepsilon - \varphi$. Hence

$$\eta_n = s_0\delta_n + \lambda_2^n(\eta - \delta s_0), \tag{B12}$$

in which λ_2^n is exponentially small compared to δ_n. Thus the average cluster size is

$$\left[\frac{df_0}{dx}\right]_{x=1} = \lim_{n\to\infty}\frac{\eta_n}{\delta_n} = s_0. \tag{B13}$$

Note that Eq. (B13) can be derived directly from Eq. (25) by linearizing it near (1,1). Neglecting exponentially small terms, we find from Eq. (B10) that

$$n \approx \ln\left(\delta_n \frac{2\varphi}{\delta/s_0 - \eta}\right) \Big/ \ln\lambda_1.$$

From (B12) we derive

$$\eta_n = s_0\delta_n + \left(\delta_n \frac{2\varphi}{\delta/s_0 - \eta}\right)^{\frac{\ln\lambda_2}{\ln\lambda_1}} (\eta - s_0\delta). \tag{B14}$$

Thus $f_0(x) = 1 - s_0(1-x) + C(1-x)^a$, where $a = \ln\lambda_2/\ln\lambda_1 > 1$ is the exponent of the highest nonanalytical term of $f(x)$ for $x \to 1$. Using Tauberian theorem we find that

$$\tau = \tau(p) = 1 + \frac{\ln\lambda_2}{\ln\lambda_1} > 2. \tag{B15}$$

Exactly at $p = p_c$ the matrix $\mathcal{A}$ cannot be diagonalized since both of its eigenvalues are equal to 1/3. Equations (B10) and (B11) acquire Jordanian form

$$\delta_n = \left(\frac{1}{3}\right)^n \delta + n/3\left(\frac{1}{3}\right)^n (\delta - \eta), \tag{B16}$$

$$\eta_n = \left(\frac{1}{3}\right)^n \eta + n/3\left(\frac{1}{3}\right)^n (\delta - \eta), \tag{B17}$$

or

$$\eta_n = \delta_n + (\eta - \delta)/3^n = \delta_n + 3\delta_n/n + o(\delta/n).$$

Inserting n from Eq. (B16), $n = \ln\delta_n/\ln 3 + o(\ln\delta_n)$, we get

$$\eta_n = \delta_n\left(1 + \frac{3\ln 3}{|\ln\delta_n|}\right) + o\left(\frac{\delta_n}{|\ln\delta_n|}\right). \tag{B18}$$

Thus at $p = p_c$ the average branch size remains finite,

$$\langle s_0\rangle = \lim_{n\to\infty}\frac{\eta_n}{\delta_n} = 1. \tag{B19}$$

Using Eq. (B18) and the Tauberian theorem we find that $\tau = 2$. However, logarithmic corrections to $F_0(s)$ now appear,

$$F_0(s) \sim \frac{1}{s^2\ln^2 s}. \tag{B20}$$

Note that the second power of the logarithm in (B20) guarantees that the average cluster size remains finite.

Below p_c the equations for δ_n, η_n become more complex:

$$\delta_n = \sqrt{q^{-n}}\left(\delta\cos\theta n - \frac{\eta - (1-\varepsilon)\delta}{\varphi}\sin\theta n\right), \tag{B21}$$

$$\eta_n = \sqrt{q^{-n}}\left(\eta\cos\theta n - \frac{(1-\varepsilon)\eta - \delta}{\varphi}\sin\theta n\right). \tag{B22}$$

It is clear that when initial values are positive ($\delta > 0$ and $\eta > 0$), δ_n must become negative for a certain value of n.

Suppose now that we know the exact solution $f_0(1)$ which corresponds to some $\eta = 1 - f_0(1)$ and $\delta = 0$. Iterating Eqs. (24) forward we find that as $m \to \infty$, $f_m(1) \to p$ and $g_m(1) \to 0$. The linearized equations (B1) and (B2) with $n = -m$ produce a sequence $\binom{\delta_m}{\eta_m}$ which follows exact solutions $1 - f_0(1)$, $1 - g_0(1) = 0$ for small m. We will try to find an approximation for η, demanding that, for certain m, $\delta_m = 1$, $\eta_m = 1 - p$:

$$\delta_m = \sqrt{q^m}\frac{\eta}{\varphi}\sin m\theta = 1, \tag{B23}$$

$$\eta_m = \sqrt{q^m}\left(\eta\cos m\theta + (1-\varepsilon)\frac{\eta}{\varphi}\sin m\theta\right) = 1 - p. \tag{B24}$$

After some algebra we get

$$m = \frac{\pi}{\theta} - \frac{1}{\theta}\arctan\frac{\varphi}{p-\varepsilon}, \tag{B25}$$

which leads to

$$\eta = \sqrt{q^{-m}}\frac{\varphi}{\sin\left(\arctan\frac{\varphi}{p-\varepsilon}\right)}. \tag{B26}$$

For p close to p_c we find that $m \sim \frac{\pi}{\theta} + O(1)$ and

$$\eta = Ce^{-\frac{A}{\sqrt{p_c - p}}}, \tag{B27}$$

in which $A = \sqrt{2}\pi \ln 3/3$. Although we made a linear approximation to the recursion, the form of the result seems to be correct as it is demonstrated in Fig. 4. The agreement is perfect over 30 orders of magnitude in f_0. Of course we do not get the correct prefactor C, but our result for A provides the correct asymptotic.

Using (B21) and (B22), we can find the average cluster size

$$\begin{aligned}\langle s_0 \rangle &= \left[\frac{d \ln f_0(x)}{dx}\right]_{x=1} = \frac{1}{f_0(1)}\left[\frac{d\eta/dn}{d\delta/dn}\right]_{n=n_0,\delta(n_0)=0} \\ &= \left(\frac{\ln q}{2}\frac{\varphi}{\theta} + 1 - \varepsilon\right) \Big/ f_0(1) \\ &\sim 3\ln 3 + 1 - C_1(p_c - p),\end{aligned} \tag{B28}$$

where C_1 is some positive constant. This equation gives the correct asymptotic behavior for $\langle s_0 \rangle$ as we can test by comparing (B28) with numerical data (see Fig. 5). Thus the average cluster size has a first order discontinuity at p_c, jumping at p_c from 1 at $p = p_c^+$ to $1+3\ln 3$ at $p = p_c^-$.

For $p < p_c$ the function $f_0(x)$ is analytical for $x \leq 1$, but has a singular derivative at $x = x_0 > 1$. In the vicinity of p_c we can find x_0 from the linearized equations (B21) and (B22) using n as a continuous parameter; thus we write $x_0 = 1 + \delta(n_0)$ where n_0 is such that

$$\left[\frac{d\delta}{dn}\right]_{n=n_0} = 0. \tag{B29}$$

Note that $\delta(n)$ approaches $\delta(n_0)$ as $\delta(n_0)+(n-n_0)^2$ while $\eta(n)$ at $n = n_0$ has nonzero derivative, $\eta(n) - \eta(n_0) \sim n - n_0$. This leads to a singularity of the type $f_0(x) = f_0(x_0) + C\sqrt{x_0 - x}$ for $f_0(x)$, suggesting that the exponent τ of the cluster size distribution is 3/2. Equation (B29) yields $x_0 = 1 + F_0(\infty)(2/e\sqrt{q}\ln q)$, which in turn gives

$$s_c \sim 1/(x_0 - 1) \sim C\exp\left(\frac{A_1}{\sqrt{p_c - p}}\right), \tag{B30}$$

implying $\sigma = 0$.

APPENDIX C: CALCULATION OF CORRELATION LENGTH

Here we show how to compute correlation lengths $\xi_\perp$ and $\xi_\parallel$ for the diode-resistor cluster on a Cayley tree. We use, as a starting point, the problem of directed percolation on a Cayley tree [10].

Correlation lengths $\xi_\perp$ and $\xi_\parallel$ can be defined as the weighted averages of the corresponding components of the radius of gyration

$$\xi_\parallel^2 = \frac{\langle R_\parallel^2 s\rangle}{\langle s\rangle} \tag{C1}$$

and

$$\xi_\perp^2 = \frac{\langle R_\perp^2 s\rangle}{\langle s\rangle}, \tag{C2}$$

where s is the number of sites in the cluster. For the directed percolation problem, we assign to each site i on a Cayley tree an integer ℓ_i that is equal to the number of bonds by which this site is connected to the origin. We will call this integer the *chemical distance.*

Assume that the Cayley tree is embedded in a d-dimensional space ($d \to \infty$) in such a way that the $d-1$ coordinates orthogonal to the direction of growth are randomly incremented by 1 or by -1 for each bond of the Cayley tree, and the coordinate parallel to the direction of growth increases by 1 for each bond leading away from the origin. Then the average square of any orthogonal coordinate for any site is equal to its chemical distance to the origin, while the square of a parallel coordinate is still equal to the square of the chemical distance.

Thus for the correlation lengths of the Cayley tree we have

$$\xi_\perp^2 = \frac{\left\langle \sum_{i=1}^{s} \ell_i \right\rangle}{\langle s\rangle} \equiv \frac{L_1}{L_0} \tag{C3}$$

and

$$\xi_\parallel^2 = \frac{\left\langle \sum_{i=1}^{s} \ell_i^2 \right\rangle}{\langle s\rangle} \equiv \frac{L_2}{L_0}. \tag{C4}$$

The size s of a finite branch of the Cayley tree that is connected to any given site is equal to

$$s = \begin{cases} 0 & \text{if initial bond of branch is not occupied} \\ 1 + s_1 + s_2 & \text{if initial bond is occupied.} \end{cases} \tag{C5}$$

Here, s_1 and s_2 are the sizes of the two branches connected to the given site. For $p > p_c$, all the branches are finite, and we can substitute Eq. (C5) by its average value

$$\langle s\rangle = (1-p)(1 + \langle s_1\rangle + \langle s_2\rangle). \tag{C6}$$

Since all branches of a Cayley tree are equivalent, we have $\langle s\rangle = \langle s_1\rangle = \langle s_2\rangle = L_0$ and we can write that

$$L_0 = (1-p)(1 + 2L_0), \tag{C7a}$$

from which we derive

$$L_0 \equiv \langle s \rangle = \frac{1-p}{2p-1}, \tag{C7b}$$

which is identical to (A13a) in Appendix A.

In order to gain a better understanding of what is happening in the diode-resistor Cayley tree, we introduce the notations L_{0i}, L_{1i}, and L_{2i}, which denote the quantities L_0, L_1, and L_2 for the branches of the simple Cayley tree that are a chemical distance i from the origin. Here the chemical distance is analogous to the level of the diode-resistor Cayley tree, but—in contrast to the actual diode-resistor Cayley tree—these quantities depend on i in a very simple way,

$$L_{0i} = L_{00}, \qquad L_{1i} = L_{10} + iL_{00}, \qquad L_{2i} = L_{20} + 2iL_{10} + i^2 L_{00}. \tag{C8}$$

In analogy with (C6) and (C7), we can write

$$L_{0i} = (1-p)(1 + 2L_{0i+1}), \tag{C9}$$

$$L_{1i} = (1-p)(i + 1 + 2L_{1i+1}), \tag{C10}$$

$$L_{2i} = (1-p)[(i+1)^2 + 2L_{2i+1}], \tag{C11}$$

or

$$L_{0n} = AL_{0n-1} - c, \tag{C12}$$

$$L_{1n} = AL_{1n-1} - cn, \tag{C13}$$

$$L_{2n} = AL_{2n-1} - cn^2, \tag{C14}$$

where $A = 1/(2-2p) > 1$ and $c = 1/2$. Iterating these equations, we find

$$L_{0n} = A^n L_{00} - \left(\sum_{i=0}^{n-1} A^i\right) c, \tag{C15}$$

$$L_{1n} = A^n L_{10} - \sum_{i=0}^{n-1} A^i (n-i)c, \tag{C16}$$

$$L_{2n} = A^n L_{20} - \sum_{i=0}^{n-1} A^i (n-i)^2 c. \tag{C17}$$

After converting the geometrical progressions in the right-hand sides, we arrive at the following form for L_{in}:

$$L_{0n} = A^n \left(L_{00} - \frac{c}{A-1}\right) + \frac{c}{A-1}, \tag{C18a}$$

$$L_{1n} = A^n \left(L_{10} - \frac{A}{(A-1)^2}c\right) + c\frac{n}{A-1} + c\frac{A}{(A-1)^2}, \tag{C18b}$$

$$L_{2n} = A^n \left(L_{20} - c\frac{A^2+A}{(A-1)^3}\right) + c\left(\frac{n^2}{A-1} + \frac{2n}{(A-1)^2} + \frac{A^2+A}{(A-1)^3}\right). \tag{C18c}$$

Now, because L_{kn} should not increase faster than the kth power of n, we must assume that the terms that contain A^n are equal to zero. This condition yields the values of L_{i0}:

$$L_{00} = \frac{c}{A-1} = \frac{(1-p)}{2p-1}, \tag{C19a}$$

$$L_{10} = \frac{cA}{(A-1)^2} = \frac{(1-p)}{(2p-1)^2}, \tag{C19b}$$

$$L_{20} = \frac{cA^2+A}{(A-1)^3} = \frac{(1-p)+2(1-p)^2}{(2p-1)^3}. \tag{C19c}$$

So for L_{00} we again derive the result of Eq. (C7b). This construction will play a crucial role in our diode-resistor calculation.

Another way of deriving (C19) is to use some identities analogous to (C5) for the quantities L_1 and L_0. This can be done if one considers a branch of $s = 1 + s_1 + s_2$ sites that has two daughter branches of sizes s_1 and s_2 growing from the site with chemical distance 1 of the parent branch

$$\sum_{j=1}^{s} \ell_j = 1 + \sum_{j=1}^{s_1} (\ell'_j + 1) + \sum_{j=1}^{s_2} (\ell'_j + 1) = s + \sum_{j=1}^{s_1} \ell'_j + \sum_{j=1}^{s_2} \ell'_j \tag{C20}$$

and

$$\sum_{j=1}^{s} \ell_j^2 = 1 + \sum_{j=1}^{s_1} (\ell'_j + 1)^2 + \sum_{j=1}^{s_2} (\ell'_j + 1)^2 = s + 2\sum_{j=1}^{s_1} \ell'_j + 2\sum_{j=1}^{s_2} \ell'_j + \sum_{j=1}^{s_1} \ell'^2_j + \sum_{j=1}^{s_2} \ell'^2_j, \tag{C21}$$

where ℓ'_j is the chemical distance in the daughter branches with respect to their origins. Averaging these two equations, we get

$$L_{10} = L_{00} + 2(1-p)L_{10}, \tag{C22a}$$

$$L_{20} = L_{00} + 4(1-p)L_{10} + 2(1-p)L_{20}, \tag{C22b}$$

which agree with the expressions of Eqs. (C19).

From Eqs. (C19) one concludes

$$\xi_\perp = \frac{1}{\sqrt{2p-1}}, \tag{C23a}$$

$$\xi_\parallel = \frac{\sqrt{3-2p}}{2p-1}, \tag{C23b}$$

which gives $\nu_\perp = 1/2$ and $\nu_\parallel = 1$, the result obtained in [10].

In solving the problem for the diode-resistor Cayley tree we will use both the ideas of Eqs. (C9)–(C11) as well as Eqs. (C7) and (C22). Because of the difference between the branches growing up and those growing down, we cannot compute the quantities L_{ki} for the branch on level i. Instead, for the diode-resistor Cayley tree, we compute the corresponding quantities d_{ki} and u_{ki} for the branches growing down and up. Now we assume $\vec{L}_{ki}$ is a vector with the components $\binom{d_{ki}}{u_{ki}}$.

Another difference of DRP and directed percolation is that now the coordinate parallel to the direction of growth is not equal to the chemical distance to the origin, but just to level i of a site. Thus we denote

$$d_{1i} = \left\langle \sum_{j=1}^{s_d} \ell_j \right\rangle, \qquad u_{1i} = \left\langle \sum_{j=1}^{s_u} \ell_j \right\rangle,$$
$$d_{2i} = \left\langle \sum_{j=1}^{s_d} i_j^2 \right\rangle, \qquad u_{2i} = \left\langle \sum_{j=1}^{s_u} i_j^2 \right\rangle \tag{C24}$$

for the branches going down and up, with sizes s_d and s_u, respectively. Here i_j is the level of the jth site and ℓ_j is its chemical distance from the origin as before. Accordingly, we will compute

$$\xi_\perp^2 = \frac{u_{20}}{u_{00}}, \qquad \xi_\parallel^2 = \frac{u_{10}}{u_{00}}. \tag{C25}$$

Another difference is that here we have a plane $i = 0$ that stops the growth downwards. These considerations lead to the important boundary conditions

$$d_{k0} = 0. \tag{C26}$$

When percolation is absent ($p > p_c$), we can use the ideas of Eq. (C6) and Eqs. (C8)–(C11) for each level of the Cayley tree and write

$$u_{0i} = (1-p)(1 + 2u_{0i+1} + d_{0i+1}),$$
$$d_{0i+1} = 2d_{0i} + u_{0i} + 1, \tag{C27}$$
$$u_{1i} = u_{0i} + (1-p)(2u_{1i+1} + d_{1i+1}), \tag{C28}$$
$$d_{1i+1} = d_{0i+1} + 2d_{1i} + u_{1i}, \tag{C29}$$
$$u_{2i} = (1-p)[(i+1)^2 + 2u_{2i+1} + d_{2i+1}],$$
$$d_{2i+1} = i^2 + 2d_{2i} + u_{2i}, \tag{C30}$$

or, in vector form,

$$\vec{L}_{0i+1} = A\vec{L}_{0i} + \vec{c}_{00}, \tag{C31}$$
$$\vec{L}_{1i+1} = A\vec{L}_{1i} + B\vec{L}_{0i} + \vec{c}_{10}, \tag{C32}$$
$$\vec{L}_{2i+1} = A\vec{L}_{2i} + \vec{c}_{22}i^2 + \vec{c}_{21}i + \vec{c}_{20}, \tag{C33}$$

in complete analogy with Eqs. (C8)–(C11). The only difference is that now $A = \begin{pmatrix} 2 & 1 \\ -1 & (q-1)/2 \end{pmatrix}$ and $B = \begin{pmatrix} 2 & 1 \\ -1 & -(q+1)/2 \end{pmatrix}$ are noncommuting matrices and $\vec{c}_{k\ell}$ are vectors, not just numbers.

1. Solution above p_c

Note that matrix A is the inverse of the matrix $\mathcal{A}$ of Eqs. (B4), and that Eq. (C27) can be obtained through logarithmic derivatives of Eqs. (18) and (19). First, in analogy with (C15) and using matrix algebra, we obtain the solution for $\vec{L}_{0n}$,

$$\vec{L}_{0n} = A^n[\vec{L}_{00} + (A-1)^{-1}\vec{c}_{00}] - (A-1)^{-1}\vec{c}_{00}. \tag{C34}$$

Note that for $p > p_c$, the matrix A has the eigenvalues λ_1^{-1} and λ_2^{-1}, one of which,

$$\lambda_1^{-1} = q/(3 - \epsilon + \varphi) = 3 - \epsilon - \varphi,$$

is less than $3 = z_c - 1$; the other,

$$\lambda_2^{-1} = q/(3 - \epsilon - \varphi) = 3 - \epsilon + \varphi,$$

is greater than $3 = z_c - 1$; note also that matrix $(A-1)^{-1}$ does not diverge at $p = p_c$.

The average size of a branch on the nth level cannot grow faster than $(z_c - 1)^n$, which is the total number of bonds of a Cayley tree of the nth order. This restriction is analogous to the restriction that L_{0n} remains finite in the directed percolation case. Here it leads to the condition that $\vec{L}_{00} + (A-1)^{-1}\vec{c}_{00}$ is parallel to the eigenvector $\vec{v}_1 = \binom{1-\epsilon+\varphi}{1}$, which corresponds to the eigenvalue λ_1. Taking into account that $d_{00} = 0$, we find that $\langle s \rangle \equiv u_{00} = 1 - \epsilon - \varphi$ for the average cluster size, exactly as before [see Eq. (B11) and those following]. The quantity u_{00} is not diverging at p_c, thus $\gamma = 0$.

Similar computations can be applied to (C30), where we find

$$\vec{L}_{2n} = A^n(\vec{L}_{20} + \vec{c}_{33}) + n^2\vec{c}_{32} + n\vec{c}_{31} + \vec{c}_{30}, \tag{C35a}$$

in which $\vec{c}_{3k}$ are some vectors not diverging at p_c. Again $\vec{L}_{20} + \vec{c}_{33}$ should be parallel to $\vec{v}_1$. This condition gives

$$u_{20} = \frac{3q-10}{q-1}(1 - \epsilon - \varphi) - \frac{5}{q-1}, \tag{C35b}$$

which remains finite at $p = p_c$ and thus, from (C25), $\nu_\perp = 0$ (see Fig. 7).

The difference comes when we solve Eqs. (C28) and (C29), which can now be written in a simpler form

$$\vec{L}_{1i+1} = A\vec{L}_{1i} + aBA^i\vec{v}_1 + \vec{c}_{40}, \tag{C36}$$

where $a\vec{v}_1 = \vec{L}_{00} + (A-1)^{-1}\vec{c}_{00}$. Note that matrices A and B do not commute and that the matrix algebra is no longer analogous to the scalar algebra. The problem can still be solved, however, if we express $aB\vec{v}_1$ as a linear

combination of the two eigenvectors

$$aB\vec{v}_1 = a_1\vec{v}_1 + a_2\vec{v}_2, \tag{C37}$$

where $\vec{v}_2 = \binom{1-\epsilon-\varphi}{1}$ is the second eigenvector of matrix A. Then we find

$$\vec{L}_{1n} = A^n\left[\vec{L}_{10} + \vec{c}_{50} + (\lambda_2^{-1} - \lambda_1^{-1})^{-1}a_2\vec{v}_2\right] + n\lambda_1^{-n}a_1\vec{v}_1 + \vec{c}_{51}, \tag{C38}$$

in which $\vec{c}_{5k}$ are vectors that are finite at $p = p_c$.

Once again, in order to prevent the unphysically rapid growth of $\vec{L}_{1n}$, we have to assume that the expression in the square brackets is parallel to $\vec{v}_1$. As before, $d_{10} = 0$ and after some calculation we get

$$u_{10} = \frac{qu_{00}}{2\varphi} + \frac{1-(q-2)u_{00}}{q-1}, \tag{C39}$$

where $u_{00} = 1 - \epsilon - \varphi$. We see that u_{10} diverges as $1/\varphi \sim (p-p_c)^{-1/2}$ when $p \to p_c^+$ (see Fig. 8) and

$$\xi_{\|} = \sqrt{\frac{u_{10}}{u_{00}}} \sim (p-p_c)^{-1/4}. \tag{C40}$$

Thus $\nu_{\|} = 1/4$ above p_c.

2. Solution below p_c

In the presence of percolation ($p < p_c$), we have to modify the form of Eqs. (C27)–(C30). The reason is that in general the probability of a site in the nth level being connected to a finite cluster through an upper bond is $[f_n(1) - p]/f_n(1)$. In the previous case when $p > p_c$, we have $f_n(1) = 1$ and we obtain Eqs. (C27)–(C30) but this is not true below p_c. Thus we have to replace the matrices A and B in Eqs. (C31)–(C33) with the level-dependent matrices A_n and B_n, which are of the form

$$A_n = \begin{pmatrix} 2 & 1 \\ -1 & (q_n-1)/2 \end{pmatrix}, \tag{C41}$$

$$B_n = \begin{pmatrix} 2 & 1 \\ -1 & -(q_n+1)/2 \end{pmatrix}, \tag{C42}$$

where we have defined

$$q_n = \frac{f_n(1)}{[f_n(1)-p]}. \tag{C43}$$

The resulting equations can be formalized as

$$\vec{L}_{k,i+1} = A_i\vec{L}_{ki} + \vec{C}_{ki}, \tag{C44}$$

in which $C_{k,i}$ are some vectors dependent on i. We divide these equations into a homogeneous and an inhomogeneous part,

$$\vec{L}_{i+1}^{(h)} = A_i\vec{L}_i^{(h)}, \quad \vec{L}_0^{(h)} = \begin{pmatrix} 0 \\ 1 \end{pmatrix}, \quad \vec{L}_n^{(h)} = \begin{pmatrix} d_n^{(h)} \\ u_n^{(h)} \end{pmatrix}, \tag{C45}$$

$$\vec{L}_{k,i+1}^{(i)} = A_i\vec{L}_{ki}^{(i)} + \vec{c}_{ki}, \quad \vec{L}_{k0}^{(i)} = \begin{pmatrix} 0 \\ 0 \end{pmatrix}, \quad \vec{L}_{kn}^{(i)} = \begin{pmatrix} d_{kn}^{(i)} \\ u_{kn}^{(i)} \end{pmatrix}. \tag{C46}$$

Then we can write

$$L_{kn} = u_{k0}\vec{L}_n^{(h)} + \vec{L}_{kn}^{(i)}. \tag{C47}$$

We use these equations for finding the behavior of u_{k0} as a function of p by applying the condition

$$\lim_{n\to\infty} u_{kn} = 0. \tag{C48}$$

This equation is true for $p < p_c$ because as n increases the probability of belonging to an infinite cluster increases. For high enough levels any upgoing bond is either blocked with probability p) or it connects to an infinite cluster. Hence the moments u_{kn} of distribution of finite branches are zero. The condition (C48) is valid only for $p < p_c$ and is equivalent to the condition for slow growth of $\vec{L}_{kn}$, $\|\vec{L}_{kn}\| \le C(z_c-1)^n$. Indeed, since $q_n \to \infty$, the largest eigenvalue of matrix A_n which corresponds to the eigenvector $\binom{0}{1}$ becomes infinite and the smallest eigenvalue that corresponds to the eigenvector $\binom{1}{0}$ approaches 2. Hence in order to grow slower than $(z_c-1)^n$, $\vec{L}_{kn}$ should be collinear to the vector $\binom{1}{0}$ which leads to Eq. (C48).

Using this limit in Eq. (C47) we arrive at the following formula for u_{k0}:

$$u_{k0} = \lim_{n\to\infty} \frac{-u_{kn}^{(i)}}{u_n^{(h)}}. \tag{C49}$$

Using (C49) we find the values of u_{k0} for $p < p_c$, that is, we iterate (C45) and (C46) using known values of $f_n(1)$ as obtained by the dichotomy method (see Appendix B). The results are presented in Figs. 5, 7, and 8 as the iteration data. The result for u_{00} is in excellent agreement with Eq. (31), which was obtained directly from the behavior of the generating function $f_0(x)$ for $x \to 1$ (see Fig. 5). We observe that for $k = 0$ and 2 both u_{k0} remain finite and as before we derive $\gamma = 0$ and $\nu_{\perp} = 0$. The story is different for u_{10} which is diverging as $|p-p_c|^{-3/2}$. This means that for $p < p_c$, $\nu_{\|} = 3/4$, thus it is different from its value above p_c, which is 1/4 (see Fig. 8). We compare the results obtained by Eq. (C49) with the direct Monte Carlo simulations of the random diode-resistor Cayley tree with a given probability p of diodes for p distant from p_c (see Fig. 2). Figures 5, 7, and 8 show the excellent agreement between the results obtained by iteration and simulation, which proves the validity of the assumptions behind our derivation of Eqs. (C45)–(C49).

We can justify the results of iterations explained above by the following analytical argument. If we bring p very close to p_c then according to Eq. (B27), $f_0(1)$ is very close to 1 and q_0 is approximately equal to $q = 1/(1-p)$, which is less than 9. Expanding Eq. (C43) we derive

$$q_n = q + q(q-1)\eta_n + O(\eta_n^2). \tag{C50}$$

If we insert η from Eq. (B26) into Eq. (B24), we see

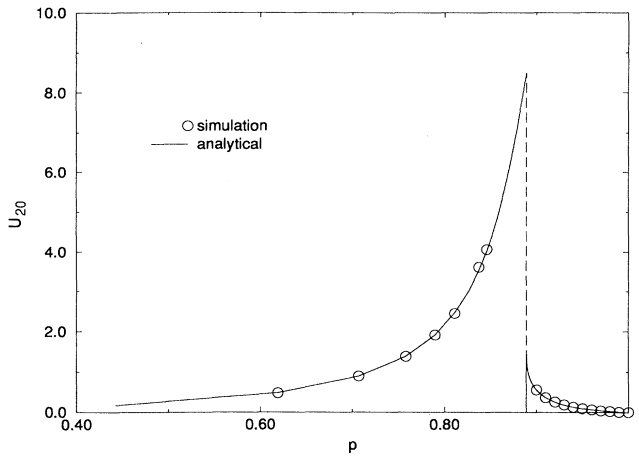

FIG. 7. Average square height u_{20} as a function of p similar to Fig. 5. The exact analytical result of Eq. (C35b) for $p > p_c$ and the numerical solution of Eqs. (C45)–(C49) for $p < p_c$ are shown by two curves that have finite limits for $p \to p_c$. The results of computer simulations on the random Cayley tree are shown by circles.

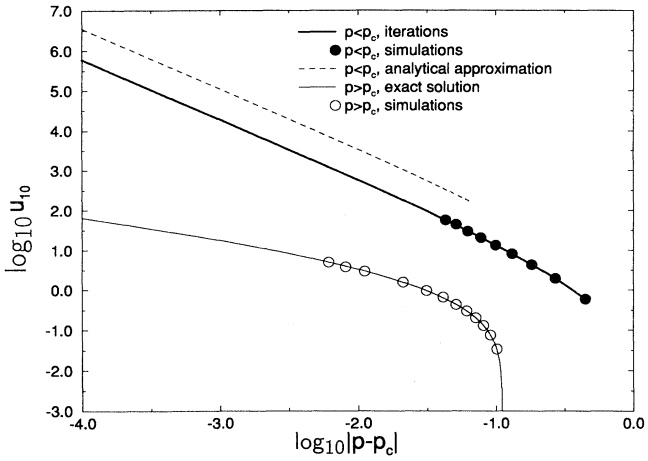

FIG. 8. The double logarithmic plot of the horizontal branch width u_{10} as a function of $|p-p_c|$ below and above p_c. The data above p_c are obtained by simulating the random diode-resistor Cayley tree (circles) as well as exact solution given by Eq. (C39) (solid line). The asymptotic slope of the analytic solution for $p \to p_c$ is $-\frac{1}{2}$. For $p < p_c$, the results of using iteration of Eqs. (C45) and (C46) in Eq. (C49) are shown by a solid line. The prediction of analytical approximation of Eqs. (C51) and (C53) inserted in (C49) is shown by a dashed line. For p close to p_c these lines become almost parallel with slope $-3/2$. The results of the Monte Carlo simulation are shown by circles.

that η_n is negligible for small n but for large enough n, η_n approaches its final value $1-p$ and q_n start to grow exponentially. At this level, the vector $\vec{C}_{kn}$, the inhomogeneous part of (C44), becomes negligible compared to the homogeneous term $A_n \vec{L}^{(i)}_{kn}$ and both $\vec{L}^{(h)}_n$ and $\vec{L}^{(i)}_{kn}$ start to diverge much faster than 3^n but their ratio u_{kn} stops changing (see Fig. 9). The value of $n = m$ when this happens can be well estimated from Eq. (B25). For $n < m$, η_n grows as 3^n and, thus, for $n < m - c\frac{\ln 1/\epsilon}{\ln 3}$, η_n becomes negligible and the behavior of Eqs. (C45) and (C46) can be again well approximated by Eqs. (C31)–(C33) with fixed matrices A and B. Thus one can expect that the limiting value of u_{kn} with $n \to \infty$ is of the same order as u_{km} when m is taken from Eq. (B25). Now we can approximate u_{km} using Eqs. (C31)–(C33), which are solvable analytically for any value of m. We iterate Eq. (C31) to get Eq. (C34) and then we can find the result by diagonalizing A as was done in Appendix B [in fact, for A^n we can use Eqs. (B21) and (B22) with $n \to -n$]. So we arrive at the following forms for $u^{(h)}_n$ and $u^{(i)}_{0n}$:

$$u^{(h)}_n = q^{n/2}\left(\cos\theta n + \frac{1-\varepsilon}{\varphi}\sin\theta n\right),$$
$$u^{(i)}_{0n} = -q^{n/2}u_{00}\frac{\sin\theta n}{\varphi}. \tag{C51}$$

Inserting $n = m$ from (B25) into (C51), we find $u_{00} = \frac{1}{1-p} = q$ which is finite (thus $\gamma = 0$), and this is of the same order as its exact value given by (B28). A quite similar analysis gives similar results for u_{20}, that is, u_{20} remains finite as $p \to p_c$. Thus $\nu_\perp = 0$ is also satisfied below p_c.

For $k = 1$ we must deal with the matrix B as we did in the case of $p > p_c$. First we iterate Eqs. (C31) and (C32) and, using Eq. (C34), arrive at

$$L^{(i)}_{1n} = A^n\left[\vec{L}^{(i)}_{10} - (A-1)^{-1}\vec{C}_{10}\right] + \sum_{i=0}^{n-1} A^i B A^{n-1-i}\vec{L}^{i}_{00} + \vec{C}_1, \tag{C52}$$

where both $\vec{L}^{i}_{00}$ and $\vec{C}_1$ are vectors of order one. Next, to solve this equation, we expand $\vec{L}^{i}_{00}$ and also $B\vec{v}_i$ in terms of the two eigenvectors $\vec{v}_1$ and $\vec{v}_2$. We eventually arrive at the following result for $u^{(i)}_{1n}$:

$$-u^{(i)}_{1n} = \frac{q^{n/2}}{2}\left\{n(3-2\epsilon)\left[\cos n\theta\left(1 - \frac{(u_{00}-1+\epsilon)(1-\epsilon)}{\varphi^2}\right) + \frac{u_{00}\sin n\theta}{\varphi}\right] + \sqrt{q}\frac{\sin n\theta}{\sin\theta}\frac{u_{00}-1-\epsilon}{\varphi^2}\right\} + \frac{q^{n/2}}{(q-1)}\left(\cos n\theta + \frac{3-q-\epsilon}{\varphi}\sin n\theta\right) + O(1). \tag{C53}$$

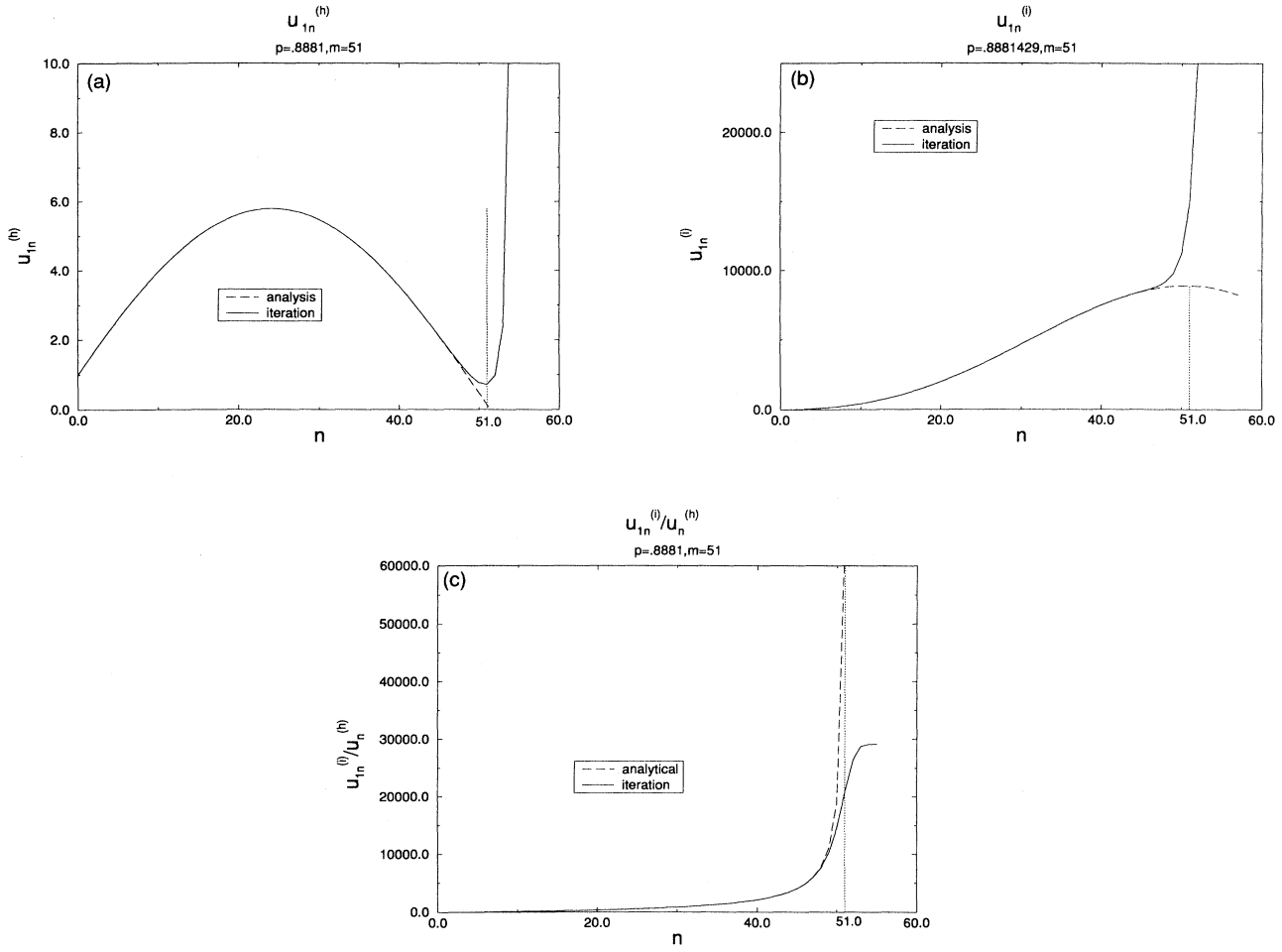

FIG. 9. (a) $u_n^{(h)}$ as a function of n for $p = 0.8881$ which is below p_c. As seen, the results of iterating Eq. (C45) (solid line) and its analytical estimate from Eq. (C51) (long dashed line) are in excellent agreement up to the value of $n = m = 51$ estimated by Eq. (B25). This value of n is shown by a vertical dotted line. Above $n = m$ the analytical value goes to zero and the iteration blows up. (b) $u_{1n}^{(i)}$ as a function of n for the same p. Again Eq. (C53) (long dashed line) estimates the numerical solution of Eq. (C46) (solid line) very accurately up to about $n = m$. (c) The ratio $u_{1n}^{(i)}/u_n^{(h)}$ which for $n = m$ estimates the value of average horizontal width u_{10} [see Eqs. (C45) and (C46) and the discussions below]. As seen, the ratio from analytical estimate Eqs. (C51), (C53) agrees with the ratio from the iteration Eqs. (C45), (C46) up to about $n = 48$. For $n = m = 51$ the analytical approximation gives a value about three times larger. Note that the ratio for numerical results quickly approaches its limiting value u_{10} for $n > m$. The ratio for analytical results computed at $n = m$ according to Eqs. (C51), (C53) diverges as $|p - p_c|^{-\frac{3}{2}}$. The numerical results remain of the same order as analytical ones since the discrepancy between them accumulates over a finite number of steps which does not increase with $p \to p_c$. The ratio of the numerical solution and the analytical approximation remains constant for different p as seen in Fig. 8.

For the m given by Eq. (B25) and a very small θ we see that $\sin m\theta$ is of order θ and $\cos m\theta$ is -1 plus terms of order θ^2. Inserting $n = m$ into the homogeneous and inhomogeneous parts we observe that the homogeneous part is finite for $n = m$ while the inhomogeneous part is proportional to m^3 or equivalently θ^{-3}. Thus $u_{10} \sim \theta^{-3} \sim |p - p_c|^{-\frac{3}{2}}$ and $\nu_\perp = \frac{3}{4}$ for $p < p_c$.

In Fig. 8 we compare the approximate analytical result (C53) with the exact numerical solutions of (C45) and (C46). The data from the Monte Carlo simulation of the diode-resistor Cayley tree are also included in Fig. 8 and verify the exactness of the iterating equations.

[1] *Surface Disordering: Growth, Roughening, and Phase Transitions*, edited by R. Jullien, J. Kertész, P. Meakin, and D. Wolf (Nova Science, New York, 1992); T. Vicsek, *Fractal Growth Phenomena*, 2nd ed. (World Scientific, Singapore, 1992); J. Krug and H. Spohn, in *Solids Far From Equilibrium: Growth, Morphology and Defects*, edited by C. Godréche (Cambridge University Press, Cambridge, England, 1991); P. Meakin, Phys. Rep. **235**, 189 (1993); T. Halpin-Healey and Y.-C. Zhang, *ibid.* **254**, 215 (1995); A.-L. Barabási and H. E. Stanley, *Fractal Concepts in Surface Growth* (Cambridge University Press, Cambridge, England, 1995).

[2] M. A. Rubio, C. A. Edwards, A. Dougherty, and J. P. Gollub, Phys. Rev. Lett. **63**, 1685 (1990); V. K. Horváth, F. Family, and T. Vicsek, J. Phys. A **24**, L25 (1991).

[3] S. Havlin, A.-L. Barabási, S. V. Buldyrev, C. K. Peng, M. Schwartz, H. E. Stanley, and T. Vicsek, in *Growth Patterns in Physical Sciences and Biology*, edited by E. Louis, L. Sander, and P. Meakin (Plenum, New York, 1992); S. V. Buldyrev, A.-L. Barabási, F. Caserta, S. Havlin, H. E. Stanley, and T. Vicsek, Phys. Rev. A **45**, R8313 (1992).

[4] S. V. Buldyrev, A.-L. Barabási, S. Havlin, J. Kertész, H. E. Stanley, and H. S. Xenias, Physica A **191**, 220 (1992).

[5] M. Kardar, G. Parisi, and Y.-C. Zhang, Phys. Rev. Lett. **56**, 889 (1986); E. Medina, T. Hwa, M. Kardar, and Y.-C. Zhang, Phys. Rev. A **39**, 3053 (1989).

[6] D. A. Kessler, H. Levine, and Y. Tu, Phys. Rev. A **43**, 4551 (1991); G. Parisi, Europhys. Lett. **17**, 673 (1992); T. Nattermann, S. Stepanow, L.-H. Tang, and H. Leschhorn, J. Phys. France II **2**, 1483 (1992); O. Narayan and D. S. Fisher, Phys. Rev. B **48**, 7030 (1993); Z. Csahók, K. Honda, and T. Vicsek, J. Phys. A **26**, L171 (1993); N. Martys, M. Cieplak, and M. O. Robbins, Phys. Rev. Lett. **66**, 1058 (1991); C. S. Nolle, B. Koiller, N. Martys, and M. O. Robbins, *ibid.* **71**, 2074 (1993).

[7] L.-H. Tang and H. Leschhorn, Phys. Rev. A **45**, R8309 (1992); K. Sneppen, Phys. Rev. Lett. **69**, 3539 (1992); H. Leschhorn and L. H. Tang, *ibid.* **70**, 2973 (1993); Z. Olami, I. Procaccia, and R. Zeitak, Phys. Rev. E **49**, 1232 (1994).

[8] L. A. N. Amaral, A. L. Barabási, and H. E. Stanley, Phys. Rev. Lett. **73**, 62 (1994); L. A. N. Amaral, A. L. Barabási, S. V. Buldyrev, S. Havlin, and H. E. Stanley, *ibid.* **72**, 641 (1994).

[9] D. Dhar, M. Barma, and M. K. Phani, Phys. Rev. Lett. **47**, 1238 (1981).

[10] B. C. Harms and J. P. Straley, J. Phys. A **15**, 1865 (1982); W. Kinzel, in *Percolation Structures and Processes*, edited by G. Deutscher, R. Zallen, and J. Adler (Hilger, Bristol, 1983).

[11] P. Meakin, P. Ramanlal, R. Ball, and L.M. Sander, Phys. Rev. A **34**, 5091 (1986).

[12] S. Redner, Phys. Rev. B **25**, 3242 (1982); in *Percolation Structures and Processes*, edited by G. Deutscher, R. Zallen, and J. Adler (Hilger, Bristol, 1983), p. 447.

[13] J. Kertész and H. J. Herrmann, J. Phys. A **18**, L1109 (1985).

[14] *Fractals and Disordered Systems*, edited by A. Bunde and S. Havlin (Springer-Verlag, Heidelberg, 1991); D. Stauffer and A. Aharony, *Introduction to Percolation Theory* (Taylor and Francis, London, 1992).

[15] S. P. Obukhov, Physica A **101**, 145 (1980).

[16] S. V. Buldyrev, S. Havlin, and H. E. Stanley, Physica A **200**, 200 (1993).

[17] S. Maslov and M. Paczuski, Phys. Rev. E **50**, R643 (1994).

[18] In (16) and (17) $\sum'$ means that the summation is not extended to the infinite cluster. The generating function approach is discussed in J. Essam, Rep. Prog. Phys. **43**, 833 (1980) and in S. Asmussen and H. Hering, *Branching Processes* (Birkhaüser, Boston, 1983).

[19] W. Feller, *An Introduction to Probability Theory and its Applications* (Wiley-Chapman, New York, 1965).

[20] It can be shown that in the general case of a Cayley tree with coordination number z_c the critical probability is given by the expression $p_c = 1 - 1/(z_c - 1)^2$.

[21] J. M. Kim and J. M. Kosterlitz, Phys. Rev. Lett. **62**, 2289 (1989).

[22] L. A. N. Amaral, A.-L. Barabási, S. V. Buldyrev, S. T. Harrington, S. Havlin, R. Sadr-Lahijany, and H. E. Stanley Phys. Rev. E **51**, 4655 (1995).

[23] S. Havlin, L. A. N. Amaral, S. V. Buldyrev, S. T. Harrington, and H. E. Stanley, Phys. Rev. Lett. **74**, 4205 (1995).

[24] H. A. Makse and L. A. N. Amaral (unpublished).